

Reproducibility of Carotid Atherosclerotic Lesion Type Characterization Using High Resolution Multicontrast Weighted Cardiovascular Magnetic Resonance

Baocheng Chu,¹ Binh An P. Phan,² Niranjana Balu,¹ Chun Yuan,¹ B. Greg Brown,² and Xue-Qiao Zhao²

Departments of Radiology,¹ and Medicine,² University of Washington Medical Center, Seattle, Washington, USA

ABSTRACT

Purpose. Cardiovascular magnetic resonance (CMR) can characterize carotid atherosclerosis. The purpose of this study is to evaluate reader agreement of carotid atherosclerotic lesion types by CMR. **Methods.** Carotid arteries of 34 patients (29 men, 5 women; mean age, 53 years) were imaged on a 1.5-T scanner. Images with 4 contrast weightings (T1, T2, proton density, and 3-dimensional time-of-flight) were acquired on each axial slice of the carotid arteries. Modified AHA criteria were used for lesion type assessment on the 4 selected axial slices (1 from the common carotid artery, 1 from the carotid bifurcation, and 2 from the internal carotid artery). The modified AHA criteria are as follows: type I-II, near-normal wall thickness without calcification; type III, diffuse wall thickening or small eccentric plaque without calcification; type IV-V, plaque with a lipid rich necrotic core surrounded by fibrous tissue with possible calcification; type VI, complex plaque with a possible surface defect, hemorrhage, or thrombus; type VII, calcified plaque; and type VIII, fibrotic plaque without a lipid core and with possible small calcifications. **Results.** Of the 272 possible axial slices (34 patients \times 2 arteries per patient \times 4 slices per artery), 256 slices were available for lesion type assessment. The majority (94%) of the lesions were of type I-II and III. κ was 0.80 and 0.60 for intra-reader and inter-reader agreement of lesion types, respectively. Inter-reader disagreement for type I-II and type III occurred in 82% of lesions. Weighted κ was 0.92 and 0.83 for intra-reader and inter-reader agreement of lesion types, respectively. **Conclusion.** The difference between type I-II and III lesions lies in the definition of the vessel wall. The moderate inter-reader agreement suggests further efforts such as establishment of normal carotid artery wall thickness by a quantitative measure are needed for carotid atherosclerotic lesion characterization.

INTRODUCTION

Recent studies linking atherosclerosis progression with clinical events have led to efforts to characterize atherosclerotic lesion types (1, 2). Research has demonstrated that complicated

lesions, such as those with carotid plaque fibrous cap rupture, are highly associated with stroke or transient ischemic attack (2). Early detection and prevention of these complicated lesions are important clinical goals.

Studies have demonstrated the ability of cardiovascular magnetic resonance (CMR) to characterize carotid atherosclerotic plaque components, such as fibrous tissue, lipid rich necrotic core, calcium, hemorrhage, thrombus, and fibrous cap thickness (3–10). Based on this capability, classification of human carotid atherosclerotic lesions using modified American Heart Association (AHA) criteria is possible with CMR (11).

Using this modified AHA criteria, a recent CMR study of hypercholesterolemic patients with moderate stenotic carotid arteries has concluded high lesion type agreement between two baseline CMR scans (12). This study implies that CMR is a reliable modality to characterize carotid atherosclerotic lesion types. However, no study has assessed reader agreement of

Received 20 July 2005; accepted 11 April 2006

Keywords: Carotid CMR, Atherosclerosis, Reproducibility.

This study is sponsored by the National Institutes of Health (RO1 HL 49546) and Merck Medical School Grant.

Correspondence to:

Baocheng Chu, MD, PhD

Departments of Radiology, Box 357115,
University of Washington Medical Center,
1959 NE, Pacific Street, Seattle,
WA 98195, USA.

fax: 206-616-9354

email: chubc@u.washington.edu

Table 1. Demographic data on the patients with coronary artery disease

Gender	
Female, n (%)	5 (15)
Male, n (%)	29 (85)
Age, range (mean), y	40–62 (53)
Ethnicity, n (%)	
Caucasian	31 (91)
Hispanic	2 (6)
Asian	1 (3)
Current smoker, n (%)	6 (17)
Hypertension, n (%)	13 (38)
Type II diabetes, n (%)	2 (6)
History of angina, n (%)	19 (55)
Prior myocardial infarction, n (%)	16 (47)
LDL-C, range, mmol/L (mean)	0.93–3.70 (2.25)
Total cholesterol, range, mmol/L (mean)	2.35–6.00 (4.06)
Triglyceride, range, mmol/L (mean)	0.39–6.88 (2.04)
HDL-C, range, mmol/L (mean)	0.46–1.29 (0.85)

carotid atherosclerotic lesion types using CMR. Such a study is essential in order to further establish the reliability of CMR to characterize atherosclerotic lesions. The aim of this study is to evaluate the reader agreement of carotid atherosclerotic lesion types using CMR.

METHODS

Patient population

As part of the High Density Lipoprotein (HDL)-Atherosclerosis Treatment Study (HATS) (13, 14), thirty-four patients (29 men, 5 women; mean age, 53 years; age range, 40–62 years, Table 1) with coronary artery disease randomly underwent carotid CMR from December 1998 to April 2000. The Institutional Review Board approved this research study and signed informed consent was obtained from each patient.

CMR imaging protocol

CMR scans were performed with a 1.5-T scanner (Signa Horizon EchoSpeed 5.8, General Electric Medical Systems, Milwaukee, Wisconsin, USA). A custom-built, phased-array carotid coil was used to improve signal-to-noise performance (15).

After an initial sagittal localizer scan, two-dimensional time-of-flight (2D TOF) angiography was performed to generate continuous axial images to identify the right and left carotid artery bifurcations. The carotid artery with the greatest degree of lumen area reduction seen on 2D TOF images was determined to be the index carotid artery. The other carotid artery with less degree of lumen area reduction (or normal lumen) was determined to be the non-index carotid artery. Based on 2D TOF images, an oblique localizer scan through the centers of the proximal internal and external carotid arteries was performed on the index carotid artery to obtain the coordinate of the carotid bifurcating point (Fig. 1).

Axial images with 4 different contrast weightings of bilateral carotid arteries were acquired using the carotid bifurcation coor-

dinate in the index artery as a landmark (Fig. 1). The four weightings included: (1) double-inversion-recovery, black-blood, fast spin-echo (FSE) T1-weighted (T1W), with 800/10/650 (repetition time msec/echo time msec [effective]/inversion time msec), and imaging duration of approximately 7 minutes; cardiac-gated, dual FSE including proton density weighted (PDW); T2-weighted (T2W), with a repetition time of three or four heartbeats per 20 msec and 40 msec echo time [effective], and imaging duration of approximately 5 minutes and three-dimensional (3D) TOF, with 23/3.8, flip angle of 25°, and imaging duration of 3 minutes.

All axial images were obtained with a field of view of 160 × 120 mm, matrix size of 256 × 256, section thickness of 2 mm, and 2 signals acquired. Section gap was 0 mm for T1W, PDW, and T2W images, and –1 mm for 3D TOF (1 mm overlapping between adjacent slices). Fat suppression was used for T1W, PDW and T2W images to reduce signals from fat adjacent to the carotid artery. The coverage of each carotid artery was 24 mm (12 slices) for T1W, 30 mm (15 slices) for PDW, and T2W, and 40 mm (40 slices) for 3D TOF images.

CMR matching and selection process

Four axial contrast-weighted images (T1W, PDW, T2W, and 3D TOF) were matched at each slice by one reviewer (B.C.) using the carotid bifurcation as a landmark for each carotid artery (Fig. 1). Although this reviewer participated in the image matching process, he was blinded to patient information and only analyzed lesion types 4 months after this process.

We chose four slices (1 from the common carotid artery, 1 from the carotid bifurcation, and 2 from the internal carotid artery) with 6 mm apart for each slice for data analysis because previous research has shown that κ analysis of lesion types, comparing adjacent locations 4 mm apart, was less than 0.20, which indicates very little dependence in lesion types (11). These slices were saved to a file for evaluating reader agreements of lesion types.

Modified AHA classification of lesion type

Modified AHA criteria (11), designed to adapt AHA criteria to carotid lesion type characterization by CMR, were used for this study. The modified AHA criteria are as follows: type I-II, near-normal wall thickness without calcification (Fig. 2); type III, diffuse wall thickening or small eccentric plaque without calcification (Fig. 3); type IV-V, plaque with a lipid rich necrotic core surrounded by fibrous tissue with possible calcification (Fig. 4); type VI, complex plaque with a possible surface defect, hemorrhage, or thrombus (Fig. 5); type VII, calcified plaque (Fig. 6); and type VIII, fibrotic plaque without a lipid core and with possible small calcifications (11).

The signal intensity of the adjacent sternocleidomastoid muscle was used as a reference to assess lesion component signal intensities as hypointense, isointense or hyperintense. Lipid rich necrotic core demonstrates isointense to hyperintense on T1W and variable signal intensity on T2W and 3D TOF images (4, 6–10). Surface defect of the carotid artery represents fibrous cap

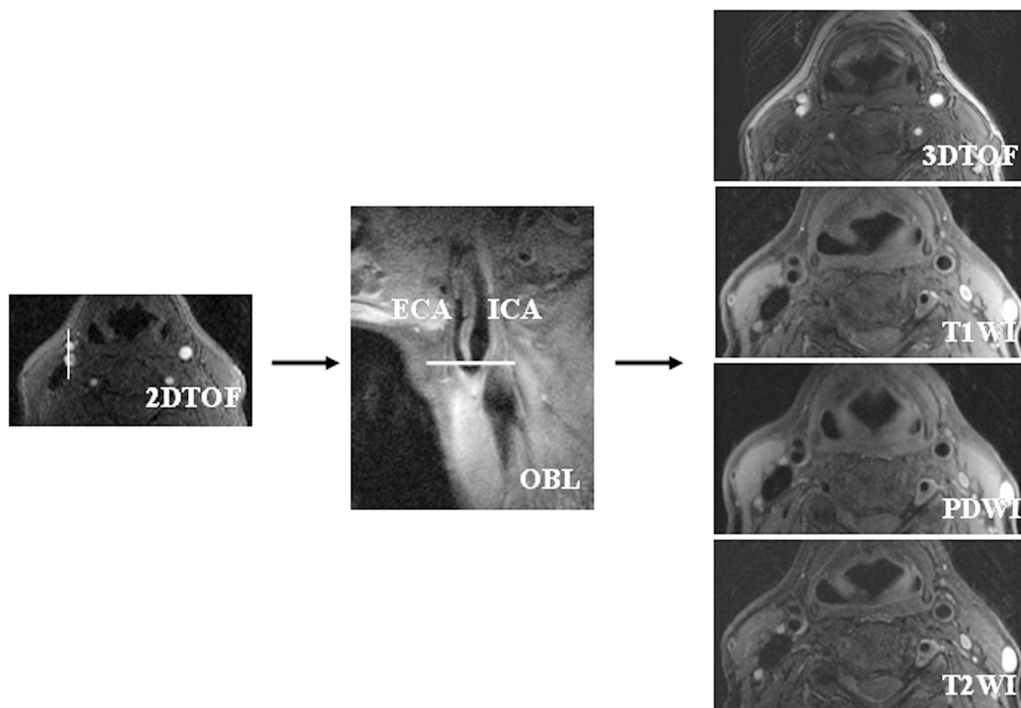


Figure 1. Steps in carotid CMR image acquisition. Axial 2D TOF image was obtained to identify the carotid artery bifurcation (vertical line). An oblique sagittal, proton density weighted fast spin echo image (double-inversion-recovery black-blood technique) shows the bifurcation (horizontal line) of the right carotid artery into the external (ECA) and internal (ICA) carotid artery (OBL). Four contrast weighted images (3D TOF, T1WI, PDWI, and T2WI) were obtained and matched using this bifurcation as a landmark. 3D TOF represents axial 3-dimensional time-of-flight image. T1WI represents axial T1-weighted image. PDWI represents axial proton density weighted image. T2WI represents axial T2-weighted image. Note that the right and left carotid artery bifurcations, for this image, are not at the same level. The axial images from the right and left carotid artery were analyzed separately.

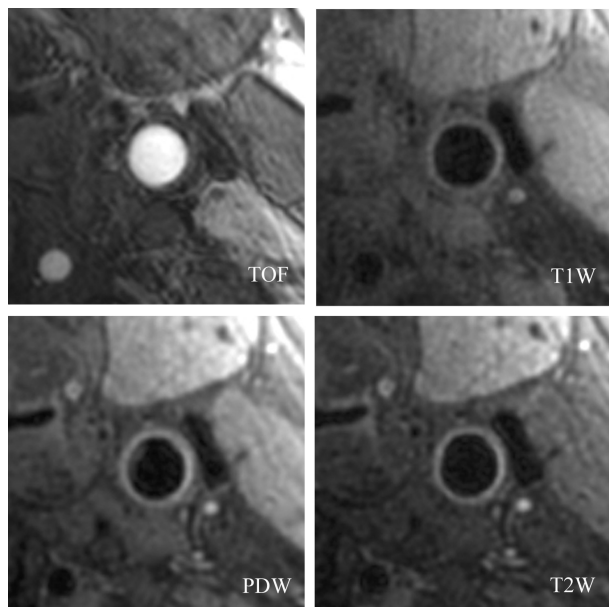


Figure 2. Lesion type I-II is shown on 4 matched weightings (3D TOF, T1WI, PDW, and T2WI). 3D TOF image shows bright blood flow in the left common carotid artery. Axial fast spin echo T1WI, PDWI, and T2WI demonstrate well defined wall, which is uniform in thickness.

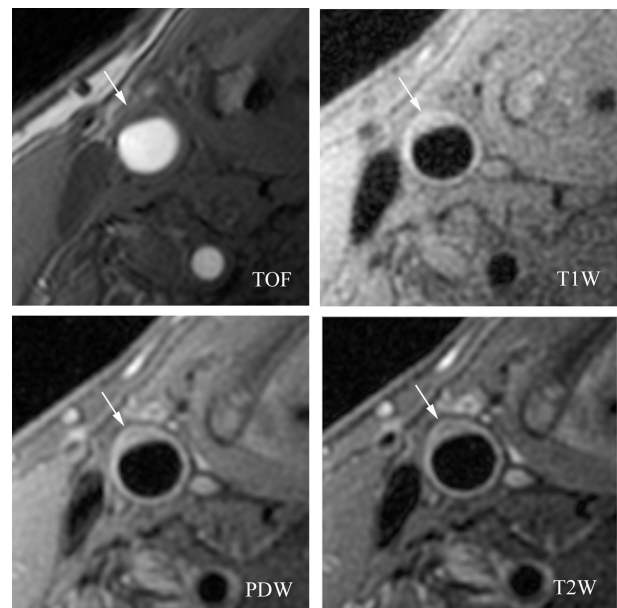


Figure 3. Lesion type III. CMR reveals small eccentric plaque (arrows) in the right common carotid artery. The plaque displays an isointense signal on 3D TOF, T1WI, PDWI, and T2WI.

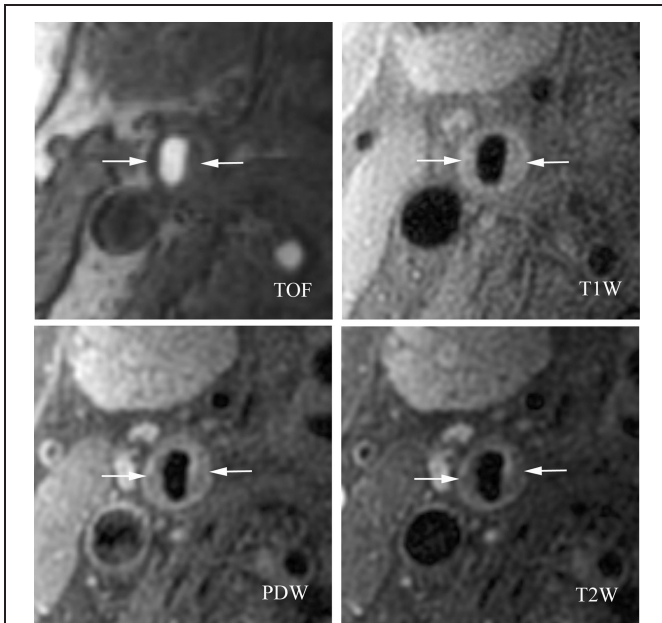


Figure 4. Lesion type IV-V. CMR reveals a lipid rich necrotic core (arrows) in the right carotid bifurcation. The plaque demonstrates isointense signal on 3D TOF, slightly hyperintense signal on T1WI, and slightly hypointense signal on PDWI, and T2WI. The carotid artery lumen is narrowed by this plaque.

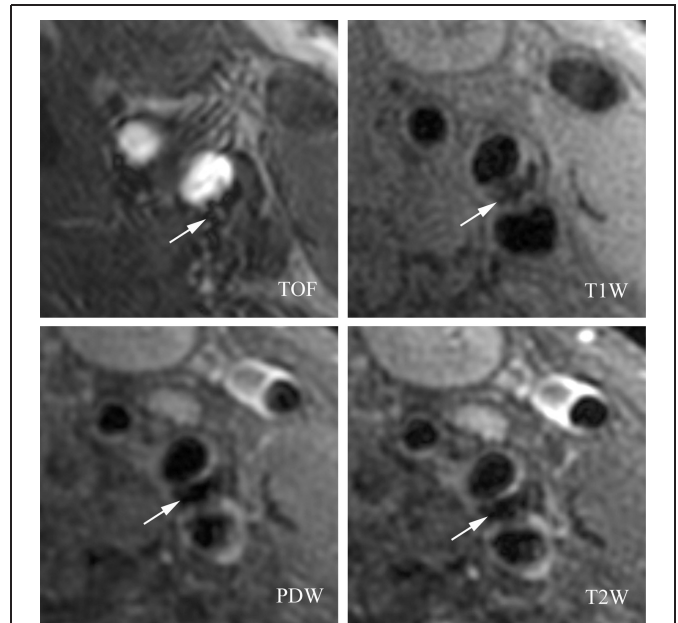


Figure 6. Lesion type VII. 3D TOF, T1WI, PDWI, and T2WI demonstrate a hypointense lesion in the left internal carotid artery. This signal feature suggests a calcified lesion (arrows) in the carotid artery wall. The signal intensity of the adjacent sternocleidomastoid muscle is used as the reference. Note that the jugular vein is located posterior to the left internal carotid artery.

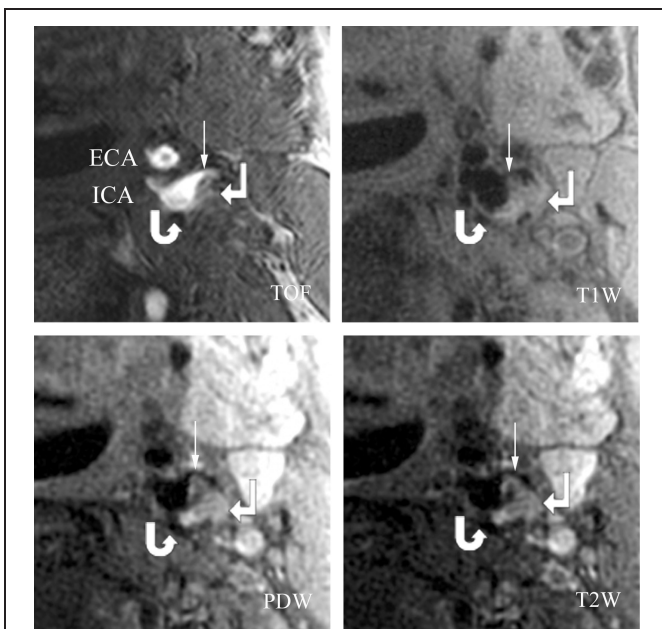


Figure 5. Lesion type VI. CMR demonstrates fibrous cap rupture (arrows), recent intraplaque hemorrhage (rectangularly curved arrows), and calcium (curved arrows) in the left internal carotid artery (ICA). The signal intensity of fibrous cap rupture is the same as that of the lumens of the left ICA and external carotid artery (ECA). Recent intraplaque hemorrhage is seen as hyperintense signal on the four weighted images (3D TOF, T1WI, PDWI, and T2WI). Calcification appears as hypointense signal on the four weighted images.

rupture, which is identified by 3D TOF as the absence of a dark band between the lumen and the plaque core and the presence of a bright gray region adjacent to the lumen correspond to recent plaque hemorrhage or mural thrombus (5, 8). Hemorrhage or thrombosis is identified by the presence of lesions with hyperintense signal on T1W and 3D TOF images and hypo- or hyperintense signal on PDW and T2W images (3, 10). Calcification is characterized by well defined areas with a hypointense signal on all four weighted images (3, 10). Loose fibrous matrix is hyperintense on PDW and T2W images, hypointense to isointense on T1W images, and isointense on 3D TOF images (10).

Lesion type review process

Lesion type was characterized by 3 separate rounds of review. Each round of review used the same, whole set of images. In the first round of review (defined as review 1), two reviewers (B.C., X.Q.Z) classified lesion type by consensus. In the second round of review (defined as review 2), two reviewers (B.C., B.P.P) also classified lesion type by consensus. In the third round of review (defined as review 3), the same two reviewers as the first round of review classified lesion type by consensus. There was an interval of 4 months between review 1 and review 2. There was an interval of 3 months between the review 2 and review 3.

Classifications of lesion type between review 1 and review 3 were compared to calculate intra-observer agreement. Classifications of lesions type between review 2 and review 3 were compared to calculate inter-observer agreement.

Analyses were made using SPSS 12.0 for Windows (SPSS Inc., Chicago, Illinois, USA).

Statistical analyses

κ and weighted κ were used to quantify the strength of agreements (16). No p values are associated with the κ and the weighted κ (16). κ was calculated as follows:

$$\kappa = (P_0 - Pe)/(1 - Pe), \quad [1]$$

where P_0 represents overall agreement and Pe represents agreement by chance. 95% confidence intervals (CIs) were calculated as follows:

$$CI_{95\%} = \kappa \pm 1.96 \cdot SE(\kappa), \quad [2]$$

where $SE(\kappa)$ represents the standard error to quantify the agreement variation.

Weighted κ , which is greater than κ when multiple categories are used, was calculated as follows:

$$\kappa(w) = [P_0(w) - Pe(w)]/[1 - Pe(w)], \quad [3]$$

where w represented weighting factor. This weighting factor can be calculated as follows:

$$w = 1 - (i - j)^2/(k - 1)^2, \quad [4]$$

where i was the number of the row, j was the number of the column, and k was the total number of categories (16).

Because multiple image slices from each artery were used for statistical evaluation, the lesion types obtained from adjacent slices were assessed for interdependency by comparison of the CMR lesion type classification of each slice with the classification of the next distal slice (“forward” κ) and the next proximal slice (“backward” κ) (11).

$\kappa < 0$ denoted poor agreement. $0 \leq \kappa \leq 0.20$ denoted slight agreement. $0.21 \leq \kappa \leq 0.40$ denoted fair agreement. $0.41 \leq \kappa \leq 0.60$ denoted moderate agreement. $0.61 \leq \kappa \leq 0.80$ denoted substantial agreement. $0.81 \leq \kappa \leq 1$ denoted almost perfect agreement (16).

RESULTS

Of the 272 possible image slices (34 patients \times 2 arteries per patient \times 4 slices per artery), 256 slices were assessed for lesion types. For some images, the bifurcations of bilateral carotid arteries were separated by many slices, which prevented the matching and analysis of images on the non-index artery. Sixteen slices on the non-index carotid arteries were thus not matched for analysis. No Type VIII lesions were observed in this study.

Intra-reader agreements of lesion types

κ for intra-reader agreement of lesion types was 0.80 (95% CI: 0.73–0.87) and weighted κ was 0.92. “forward” κ was 0.16.

Table 2. Intra-reader agreement of carotid atherosclerotic lesion types

		Review 1					
		I-II	III	IV-V	VI	VII	Total
Review 3	I-II	82	8	0	0	0	90
	III	15	135	2	0	0	152
	IV-V	0	2	4	0	0	6
	VI	0	0	0	3	0	3
	VII	0	0	0	0	5	5
	Total	97	145	6	3	5	256

Review 1 and review 3 were performed by the same two reviewers. Comparison between both readings generates intra-reader agreement. κ is 0.80 (95% confidence interval: 0.73–0.87) and weighted κ is 0.92 for intra-reader agreement of carotid atherosclerotic lesion types using modified AHA criteria on CMR (11).

“backward” κ was 0.05. For review 1, the lesion type percentage was 38%, 57%, 2%, 1%, and 2% for type I-II, III, IV-V, VI, and VII, respectively. For review 3, the lesion type percentage was 35%, 59%, 2%, 1%, and 2% for type I-II, III, IV-V, VI, and VII, respectively.

Intra-reader disagreement of lesion types occurred in 27 (10%) out of 256 lesions. Among these 27 lesions, 23 (85%) involved disagreement between type I-II and III, and four (15%) between type III and IV-V (Table 2).

Inter-reader agreements of lesion types

κ for inter-reader agreement of lesion types was 0.60 (95% CI: 0.50–0.69) and weighted κ was 0.83. “Forward” κ was 0.05. “Backward” κ was 0.07. For review 2, the percentage was 27%, 68%, 2%, 0.3%, and 2% for lesion type I-II, III, IV-V, VI, and VII, respectively.

Inter-reader disagreement of lesion types occurred in 51 (20%) out of 256 lesions. Among these 51 lesions, 42 (82%) involved disagreement between type I-II and III, and 6 (12%) between type III and IV-V (Table 3).

Table 3. Inter-reader agreement of carotid atherosclerotic lesion types

		Review 2					
		I-II	III	IV-V	VI	VII	Total
Review 3	I-II	59	31	0	0	0	90
	III	11	137	3	0	1	152
	IV-V	0	3	3	0	0	6
	VI	0	2	0	1	0	3
	VII	0	0	0	0	5	5
	Total	70	173	6	1	6	256

Review 2 and review 3 were performed by different reviewers. Comparison between both readings generates inter-reader agreement. κ is 0.60 (95% confidence interval: 0.50–0.69) and weighted κ is 0.83 for inter-reader agreement of carotid atherosclerotic lesion types using modified AHA criteria on CMR (11).

DISCUSSION

Previous research has demonstrated that the classification of human carotid atherosclerotic lesions is possible with CMR (11). Overall, lesion type classifications obtained by carotid CMR showed good agreement with histology, with κ (95% CI) of 0.74 (0.67–0.82) and weighted κ of 0.79. Using location-matched histology sections as reference, CMR classification of lesion types revealed the following sensitivity and specificity: type I-II lesions, 67% and 100%; type III lesions, 81% and 98%; type IV-V lesions, 84% and 90%; type VI lesions, 82% and 91%; type VII lesions, 80% and 94%; and type VIII lesions, 56% and 100% (11).

In the modified AHA classification, types I and II lesions were combined into type I-II because the current resolution of CMR does not allow for the differentiation of discrete foam cells in type I and the multiple foam cell layers of the fatty streak in type II. Types IV and V were combined into type IV-V because of the inability of CMR to distinguish the proteoglycan composition of the type IV cap versus the dense collagen of the type V cap (11).

Our study demonstrates substantial intra-reader agreement in the classification of lesion type. The weighted κ is greater than the unweighted κ , which may reflect the actual agreement better than does the unweighted κ in this study (16).

We found moderate inter-reader agreement in the classification of lesion type. Inter-reader disagreement of lesion types occurred in 51 (20%) out of 256 lesions. Among these 51 lesions, 42 (82%) involved disagreement between type I-II and III. This disagreement is a major reason for the moderate inter-reader agreement as lesion types I-II and III accounted for 94% and 95% of the total lesion types recorded by review 2 and review 3, respectively.

According to this modified AHA criteria, lesion type III can be diffuse wall thickening or eccentric plaque. As there is no established CMR standard for normal carotid artery wall thickness, distinction between diffuse wall thickening and “near normal” wall thickness (type I-II) is difficult. To improve reader agreement, especially for types I-II and III, future CMR studies are needed by a quantitative measure to establish normal standards for carotid artery wall thickness.

We did not find any type VIII lesions in this study. Lesion type VIII represents highly fibrotic lesions that are often associated with severe carotid artery stenosis (1), which was absent in our patient population.

This study was analyzed on the basis of individual CMR slices, rather than by individual carotid arteries. By this analysis method, CMR has shown to be able to characterize different lesion components such as plaque rupture, hemorrhage, and lipid core (3–10). Research has demonstrated that complicated lesions, such as those with carotid plaque fibrous cap rupture, are highly associated with stroke or transient ischemic attack (2). Analysis on a per vessel basis may potentially ignore details of tissue characterization (17, 18). Furthermore, κ analysis of interdependency among adjacent slices was ≤ 0.16 for both forward and backward κ . This indicates

that interdependency among adjacent slices is small in this study.

Although there is fair amount of interval between the three reviews, some concerns regarding the blindness still exist since one reader participated in all three reviews in this study. A more strict measure for review process would ensure more reliable assessment of lesion types in our future study.

In this study, we did not conduct direct correlation between carotid artery lesion types and coronary artery disease. Current CMR studies are underway to evaluate the association of carotid and coronary artery disease.

CONCLUSION

The difference between type I-II and III lesions lies in the definition of the vessel wall. The moderate inter-reader agreement suggests further efforts such as establishment of normal carotid artery wall thickness by a quantitative measure are needed for carotid atherosclerotic lesion characterization.

ACKNOWLEDGEMENT

We thank Andrew Ho for editing this manuscript.

REFERENCES

1. Stary HC, Chandler AB, Dinsmore RE, Fuster V, Glagov S, Insull W Jr, et al. A definition of advanced types of atherosclerotic lesions and a histological classification of atherosclerosis. A report from the Committee on Vascular Lesions of the Council on Arteriosclerosis, American Heart Association. *Circulation* 1995;92:1355–1374.
2. Yuan C, Zhang SX, Polissar NL, Echelard D, Ortiz G, Davis JW, et al. Identification of fibrous cap rupture with magnetic resonance imaging is highly associated with recent transient ischemic attack or stroke. *Circulation* 2002;105:181–185.
3. Chu B, Kampschulte A, Ferguson MS, Kerwin WS, Yarnykh VL, O'Brien KD, et al. Hemorrhage in the atherosclerotic carotid plaque: a high resolution CMR study. *Stroke* 2004;35:1079–1084.
4. Yuan C, Mitsumori LM, Ferguson MS, Polissar NL, Echelard D, Ortiz G, et al. In vivo accuracy of multispectral magnetic resonance imaging for identifying lipid-rich necrotic cores and intraplaque hemorrhage in advanced human carotid plaques. *Circulation* 2001;104:2051–2056.
5. Mitsumori LM, Hatsukami TS, Ferguson MS, Kerwin WS, Cai JM, Yuan C. In vivo accuracy of multisequence MR imaging for identifying unstable fibrous caps in advanced human carotid plaques. *J Magn Reson Imaging* 2003;17:410–420.
6. Toussaint JF, LaMuraglia GM, Southern JF, Fuster V, Kantor HL. Magnetic resonance images lipid, fibrous, calcified, hemorrhagic, and thrombotic components of human atherosclerosis in vivo. *Circulation* 1996;94:932–938.
7. Fayad ZA, Fuster V. Characterization of atherosclerotic plaques by magnetic resonance imaging. *Ann N Y Acad Sci* 2000;902:173–186.
8. Hatsukami TS, Ross R, Polissar NL, Yuan C. Visualization of fibrous cap thickness and rupture in human atherosclerotic carotid plaque in vivo with high-resolution magnetic resonance imaging. *Circulation* 2000;102:959–964.

9. Yuan C, Mitsumori LM, Beach KW, Maravilla KR. Carotid atherosclerotic plaque: noninvasive MR characterization and identification of vulnerable lesions. *Radiology* 2001;221:285–299.
10. Saam T, Ferguson MS, Yarnykh VL, Takaya N, Xu D, Polissar NL, et al. Quantitative evaluation of carotid plaque composition by in vivo CMR. *Arterioscler Thromb Vasc Biol* 2005;25:234–239.
11. Cai JM, Hatsukami TS, Ferguson MS, Small R, Polissar NL, Yuan C. Classification of human carotid atherosclerotic lesions with in vivo multicontrast magnetic resonance imaging. *Circulation* 2002;106:1368–1373.
12. Chu B, Hatsukami TS, Polissar NL, Zhao XQ, Kraiss LW, Parker DL, et al. Determination of carotid artery atherosclerotic lesion type and distribution in hyperlipidemic patients with moderate carotid artery stenosis using non-invasive magnetic resonance imaging. *Stroke* 2004;35:2444–2448.
13. Brown BG, Albers JJ, Chait A, Frohlich J, Cheung MC, Heise N, et al. Lipid altering or antioxidant vitamins for patients with coronary disease and very low HDL cholesterol? The HDL-Atherosclerosis Treatment Study design. *Can J Cardiol* 1998;14:6–13.
14. Brown BG, Zhao XQ, Chait A, Fisher LD, Cheung MC, Morse JS, et al. Simvastatin and niacin, antioxidant vitamins, or the combination for the prevention of coronary disease. *N Engl J Med* 2001;345:1583–1592.
15. Hayes C, Mathis CM, Yuan C. Surface coil phased arrays for high-resolution of the carotid arteries. *J Magn Reson Imaging* 1996;6:109–112.
16. Kundel HL, Polansky M. Measurement of observer agreement. *Radiology* 2003;228:303–308.
17. Naghavi M, Libby P, Falk E, Casscells SW, Litovsky S, Rumberger J, et al. From vulnerable plaque to vulnerable patient: a call for new definitions and risk assessment strategies: Part I. *Circulation* 2003;108:1664–1772.
18. Naghavi M, Libby P, Falk E, Casscells SW, Litovsky S, Rumberger J, et al. From vulnerable plaque to vulnerable patient: a call for new definitions and risk assessment strategies: Part I. *Circulation* 2003; 108:1772–1778.